



Published in final edited form as:

J Nucl Med. 2010 April ; 51(4): 632–638. doi:10.2967/jnumed.109.071233.

High ^{18}F -fluorodeoxyglucose (^{18}F -FDG) uptake in microscopic peritoneal tumors requires physiological hypoxia

Xiao-Feng Li^{1,2,3,*}, Yuanyuan Ma⁴, Xiaorong Sun^{1,5}, John L. Humm¹, C. Clifton Ling¹, and Joseph A. O'Donoghue¹

¹ Department of Medical Physics, Memorial Sloan-Kettering Cancer Center, New York, NY

² Department of Nuclear Medicine, The Second Affiliated Hospital of Harbin Medical University, Harbin, Heilongjiang, China

³ Imaging Center, The Fourth Affiliated Hospital of Harbin Medical University, Harbin, Heilongjiang, China

⁴ Department of Pathology, Memorial Sloan-Kettering Cancer Center, New York, NY

⁵ Department of Nuclear Medicine, PET-CT Center, Shandong Cancer Hospital and Institute, Jinan, Shandong, China

Abstract

The objective of this study was to examine ^{18}F -fluorodeoxyglucose (^{18}F -FDG) uptake in microscopic tumors grown intraperitoneally in nude mice and to relate this to physiological hypoxia and glucose transporter-1 (GLUT-1) expression.

Methods—Human colon cancer HT29 and HCT-8 cells were injected intraperitoneally into nude mice to generate disseminated tumors of varying sizes. Following overnight fasting, animals, either breathing air or carbogen (95% O_2 + 5% CO_2), were intravenously administered ^{18}F -FDG together with the hypoxia marker pimonidazole (PIMO) and the cellular proliferation marker bromodeoxyuridine (BrdUrd) one hour before sacrifice. Hoechst 33342, a perfusion marker, was administered one minute before sacrifice. Following sacrifice, the intratumoral distribution of ^{18}F -FDG was assessed by digital autoradiography of frozen tissue sections. This was compared with the distributions of PIMO, GLUT-1 expression, BrdUrd and Hoechst 33342 as visualized by immunofluorescent microscopy.

Results—Small tumors (< 1 mm diameter) had high ^{18}F -FDG accumulation and were severely hypoxic with high GLUT-1 expression. Larger tumors (1–4 mm diameter) generally had low ^{18}F -FDG accumulation and were not significantly hypoxic with low GLUT1 expression. Carbogen breathing significantly decreased ^{18}F -FDG accumulation and tumor hypoxia in microscopic tumors but had little effect on GLUT1 expression.

Conclusion—There was high ^{18}F -FDG uptake in microscopic tumors which was spatially associated with physiological hypoxia and high GLUT-1 expression. This enhanced uptake was abrogated by carbogen breathing, indicating that in the absence of physiological hypoxia, high GLUT1 expression, by itself, was insufficient to ensure high ^{18}F -FDG uptake.

Keywords

micrometastasis; glucose metabolism; hypoxia; ^{18}F -fluorodeoxyglucose; autoradiography

*Corresponding author: Xiao-Feng Li, M.D., PhD., Department of Diagnostic Radiology, University of Louisville School of Medicine, 530 S. Jackson Street, CCB-C07, Louisville KY 40202. Phone: (502)-852-3401; Fax: (502)-852-1754; xiao-feng.li@louisville.edu. First author Dr. Xiao-Feng Li is not in training

Introduction

^{18}F -fluorodeoxyglucose (^{18}F -FDG) positron emission tomography (PET) imaging has emerged as an important clinical tool for cancer detection, staging, and monitoring of response and is routinely used in the clinical management of several cancer types (1). The uptake of ^{18}F -FDG, an analog of glucose, is largely proportional to the rate of glucose metabolism enabling this parameter to be quantified (2). In hypoxic conditions, cancer cells may undergo a switch from aerobic to anaerobic glucose metabolism. This adaptive response involves the coordinated expression of many hypoxia inducible factor (HIF)-regulated proteins, such as GLUT-1, and various glycolytic enzymes (3). Glucose metabolism in hypoxic cancer cells has been studied in cell culture and in animal models of macroscopic tumors [reviewed in (2)]; however results have been mixed and controversial (4–14).

We have previously shown in an animal model of disseminated peritoneal disease derived from HT29 and HCT-8 colorectal cancer cells (15,16) that microscopic tumors (less than 1 mm diameter) were poorly perfused and intensely hypoxic. In contrast, larger tumors (approx. 1–4 mm diameter) were well-perfused and not significantly hypoxic. We also found that hypoxia in microscopic peritoneal tumors could be substantially reduced by having animals breathe carbogen (95% O_2 +5% CO_2) (15,16). Glucose metabolism in microscopic tumors and its relation to hypoxia has not yet been investigated.

Non-invasive PET imaging is impractical for directly assessing ^{18}F -FDG uptake in individual microscopic tumors, which are too small to be seen (16). However, such models may still provide a useful means of examining the relationship between radiotracer distribution and the features of microscopic tumors, including their hypoxic status. Digital autoradiographic (DAR) detection systems can quantitatively determine the spatial distribution of radioactivity with a pixel resolution of 25–50 μm . The spatial distributions of microenvironmental variables such physiological hypoxia, upregulated protein expression, blood perfusion and cellular proliferation can be visualized on tumor sections by immunofluorescence methods (17). In addition, the disseminated peritoneal disease model provides a diversity of tumors of differing size and hypoxic status growing in the same animal, thereby reducing or eliminating issues associated with inter-animal variability.

In the current study, we report for the first time the use of correlative imaging methodologies to examine the uptake of ^{18}F -FDG in microscopic tumors and relate this to hypoxic status. ^{18}F -FDG uptake, visualized by DAR at 50 μm pixel resolution, was compared with immunofluorescent visualization of pimonidazole binding and GLUT-1 expression. We also report on how ^{18}F -FDG uptake in microscopic tumors is altered by carbogen breathing.

Materials and Methods

Tumor cell lines and animals

Two human cancer cell lines were used in experiments: HT29 and HCT-8; both originally derived from colorectal adenocarcinomas. Cancer cell lines were purchased from American Type Cell Collection (Manassas, VA). HT29 and HCT-8 cells were maintained in McCoy's 5A modified medium (Gibco, Grand Island, NY) and RPMI 1640 medium (Cellgro, Herndon, VA), respectively. All media were supplemented with 10% fetal bovine serum (Gemini, West Sacramento, CA), 1% glutamine and 1% antibiotic mixture (Cellgro). Cells were grown at 37°C in a humidified 5% CO_2 incubator. Exponentially growing cells were harvested with 0.05% trypsin *plus* EDTA for HT29 and 0.25% trypsin *plus* EDTA (Cellgro)

for HCT-8, washed and suspended in phosphate buffered saline (PBS). The number of cells was counted using a Coulter counter (Beckman-Coulter, Miami, FL).

All experiments were performed using 6–8 week old female athymic NCr-*nu/nu* mice purchased from NCI-Frederick Cancer Research Institute (Bethesda, MD). Nude mice were maintained and used according to institutional guidelines. The experimental protocols were approved by the Institutional Animal Care and Use Committee. Animals were housed five *per* cage and kept in the institutional small animal facility at a constant temperature and humidity. Food pellets and water were provided *ad libitum*.

Establishment of Microscopic Tumors in Animals

Microscopic peritoneal tumors

Disseminated microscopic tumors were generated in the peritoneum as previously described (15,16), briefly, $5\text{--}10 \times 10^6$ cells/0.1–0.2 ml of cancer cell suspensions were injected intraperitoneally into unanesthetized mice and experiments were performed typically 6–7 weeks (HT29) or 3–4 weeks (HCT-8) later. At these times, distributions of tumors ranging from a few hundred micrometers up to several millimeters in diameter were observed to be present on or in the intestinal serosa.

HT29 Ascites tumors

At the time of sacrifice, ascites was evident in the majority of animals injected intraperitoneally with HT29 cells. The ascites fluid was observed to be bloody and contained a distribution of free-floating tumor cell aggregates of sizes up to 1 mm in diameter, denoted here as *ascites tumors*. HT29 ascites tumors were typically ellipsoidal in shape with the appearance of duct-like structures in the interior.

Experimental procedures

The hypoxia marker, pimonidazole hydrochloride (1-[(2-hydroxy-3-piperidinyl)propyl]-2-nitroimidazole hydrochloride) (Chemicon International, Temecula, CA) was dissolved in physiological saline at a concentration of 20 mg/ml. The proliferation marker, bromodeoxyuridine (BrdUrd, Roche Diagnostics, Indianapolis, IN) was first dissolved in DMSO and further diluted in physiological saline to a final concentration of 20 mg/ml. The blood perfusion marker, Hoechst 33342 (Sigma-Aldrich, St. Louis, MO) was dissolved in physiological saline at a concentration of 5 mg/ml. In all cases, fresh drug solutions were prepared on the day of injection.

All animals were fasted overnight before experiments which were performed without anesthesia. Mice were injected via the tail vein with a mixture of ^{18}F -FDG (7.4–13.3 MBq), pimonidazole (2 mg) and BrdUrd (4 mg) 1 hour before sacrifice (total injection volume 0.4 ml). Hoechst 33342 (0.5 mg, 0.1 ml) was injected via the tail vein 1 min before sacrifice. For experiments featuring carbogen breathing, mice were placed in a plastic chamber (20 × 10 × 10 cm) into which carbogen (95% O₂; 5% CO₂) was delivered at a flow rate of 5 L/min (15). After one hour of breathing carbogen, animals were injected with the ^{18}F -FDG/pimonidazole/BrdUrd mixture described above then returned to the carbogen chamber for another hour prior to Hoechst 33342 administration and sacrifice.

In total, ^{18}F -FDG uptake in disseminated HT29 peritoneal tumors was examined in 7 air-breathing and 4 carbogen-breathing animals, and in 2 air-breathing and 2 carbogen-breathing animals with disseminated HCT-8 peritoneal tumors.

Preparation of frozen tumor sections

Immediately after animal sacrifice, tumor tissues or ascites fluid were removed for subsequent processing. Peritoneal tumors (adhering to the intestinal serosa) were washed with cold PBS to remove any attached ascites tumors before freezing and embedding in optimal cutting tissue medium (OCT, 4583, Sakura Finetek, Torrance CA). Ascites tumors were harvested, washed with cold PBS to remove red blood cells, frozen and embedded in OCT. Immediately thereafter, 5 contiguous 8 μm -thick tissue sections were cut using a Microm HM500 cryostat microtome (Microm International GmbH, Walldorf, Germany) and adhered to poly-L-lysine coated glass microscope slides (Polysciences, Inc. Warrington, PA).

^{18}F -FDG digital autoradiography (DAR)

As described previously (18), autoradiograms were obtained by placing the tumor sections in a film cassette against a Fujifilm BAS-MS2325 imaging plate (Fuji Photo Film Co, Tokyo, Japan). Plates were exposed overnight, and read by a Fujifilm BAS-1800II bio-imaging analyzer (Fuji Photo Film Co) which generated digital images with pixel dimensions of 50 μm \times 50 μm . DAR image intensity was expressed in the machine readout parameter of photostimulable luminescence per square mm (PSL/ mm^2) and was quantified using Multi Gauge software (version 2.2, Fujifilm). Subsequently the derived PSL/ mm^2 values were converted to MBq/g based on the known start and end times of the DAR exposure and a previously measured system calibration factor of 103 PSL/ mm^2 per MBq hr/g (18). Finally tumor uptakes were expressed in terms of percentage injected dose per gram based on the known administered activities.

Visualization of Pimonidazole, GLUT-1, BrdUrd, Hoechst 33342 and H&E on tumor sections

Images of the distributions of pimonidazole, GLUT-1, BrdUrd and Hoechst 33342 were obtained after completion of ^{18}F -FDG DAR exposures as described previously (15). In order to minimize issues associated with section alignment and registration, the same tumor section used for DAR or contiguous adjacent sections were used for all images. Briefly, slides were air-dried, fixed in cold acetone (4°C) for 20 min, and incubated with SuperBlock (#37515, Pierce Biotechnology, Rockford, IL) at room temperature for 30 min. All antibodies were also applied in SuperBlock. Sections were then incubated with FITC conjugated anti-pimonidazole monoclonal antibody (Chemicon International), diluted 1:25, for one hour at room temperature. GLUT-1 staining was performed either on the same or adjacent section to that stained for pimonidazole by incubating for one hour at room temperature with rabbit anti-GLUT-1 polyclonal antibody (Millipore) diluted 1:50. Sections were washed three times in PBS, each wash lasting five minutes, and incubated for one hour at room temperature with either AlexaFluor568- (for sections co-stained with pimonidazole) or AlexaFluor488-conjugated goat anti-rabbit antibody (1:100, Molecular Probes, Eugene, OR) and washed again. For BrdUrd staining, adjacent sections to those used for pimonidazole were treated with 2N HCl for 10 minutes at room temperature followed by 0.1M Borax for 10 minutes at room temperature. Sections were then exposed to AlexaFluor594-conjugated anti-BrdUrd antibody (1:20 dilution, Molecular Probes, Eugene, OR) for one hour at room temperature, and washed. To control for nonspecific binding of antibodies, stained sections were processed from similar tumors that had not been exposed to pimonidazole or BrdUrd. Controls for GLUT-1 staining consisted of sections where primary antibody was omitted. Images were acquired at $\times 100$ magnification using an Olympus BX40 fluorescence microscope (Olympus America Inc., Melville, NY) equipped with a motorized stage (Prior Scientific Instruments Ltd., Cambridge, UK). Hoechst 33342

and pimonidazole were imaged using blue and green filters respectively. GLUT-1 was imaged using a red or green filter depending on the fluorophore used (as described above) and BrdUrd was imaged using a red filter. After acquisition of fluorescence images, tumor sections were stained with hematoxylin and eosin (H&E) and imaged by light microscopy. Microscopic images were co-registered and analyzed using Adobe Photoshop 7.0 (Adobe, San Jose, CA).

Statistical analysis

Statistical significance was examined by two-tailed Student's t-test. P value less than 0.05 was considered as statistically significant difference.

Results

^{18}F -FDG uptake in disseminated peritoneal disease arising from HT29 tumor cells was studied in 7 air-breathing animals. In all cases results were broadly similar. Figure 1 shows a representative example of the relationship between ^{18}F -FDG uptake and pimonidazole binding, GLUT-1 expression, cellular proliferation (as visualized by BrdUrd incorporation) and blood perfusion (as visualized by Hoechst 33342). In general, there was spatial co-localization between high levels of ^{18}F -FDG uptake, pimonidazole binding and GLUT-1 expression. Such regions tended to correspond to low levels of cellular proliferation and blood perfusion. In particular, the smallest tumor deposits (<1 mm diameter) were hypoxic (as evidenced by high pimonidazole binding) and had high ^{18}F -FDG uptake. In these tumors GLUT-1 expression was high, BrdUrd staining was confined to the rim and blood perfusion was minimal. Larger tumors (~1–4 mm diameter) were not hypoxic (low pimonidazole binding) and displayed relatively low ^{18}F -FDG uptake and GLUT-1 expression. Additionally, BrdUrd-positive cells were distributed throughout the larger tumors and blood perfusion was relatively high. Figure 2 shows quantitative ^{18}F -FDG uptake in a collection of peritoneal HT29 tumors from a single air-breathing mouse [5 tumors (<1mm) and 4 tumors (1–4mm)]. ^{18}F -FDG uptake was significantly greater in the sub-millimeter tumors than in the larger ones.

Two air-breathing animals with disseminated peritoneal disease arising from HCT-8 tumor cells were also studied. The results in this case were similar to those for HT29 tumors. An example is shown in Suppl. Fig. 1.

Figure 3 shows an example of HT29 ascites tumors. These resembled the microscopic peritoneal tumors, in that they had high ^{18}F -FDG uptake, pimonidazole binding and GLUT-1 expression throughout with BrdUrd positivity seen only in the rim.

Figure 4 illustrates the differences in ^{18}F -FDG uptake in disseminated peritoneal HT29 microscopic tumors (< 1mm diameter) between air- and carbogen-breathing conditions. A total of four animals from 2 independent experiments were studied with carbogen breathing and in all cases results were broadly similar. For example, in an experiment which included 2 carbogen-breathing mice and 2 air-breathing mice, following two hours of carbogen breathing (one hour before and one hour after ^{18}F -FDG administration), there was a major reduction in ^{18}F -FDG uptake in microscopic tumors comparing with that for air breathing animals. The histogram of figure 4D is based on data from a total of 9 tumors (<1mm) from 2 air-breathing animals and 11 tumors (<1mm) from 2 carbogen-breathing animals. ^{18}F -FDG tumor uptake was significantly reduced for the carbogen-breathing animals.

We also attempted to quantify the degree of immunohistochemical staining based on mean fluorescence intensity. For pimonidazole, there was also an apparent decrease in binding for carbogen breathing (mean fluorescence intensity 82 ± 9 , $n = 11$ microscopic tumors from 2

mice) in comparison to air breathing (mean fluorescence intensity 186 ± 16 , $n = 9$ microscopic tumors from 2 mice). Taking these numerical values at face value the difference was statistically significant ($p < 0.001$). In contrast, the level of GLUT-1 expression quantified by fluorescence intensity in microscopic tumors was not significantly different between carbogen breathing (153 ± 24 , $n = 11$) and air breathing condition (151 ± 22 , $n = 9$) ($p = 0.84$). However it should be noted that the linearity of the relationship between fluorescence intensity and antigen concentration is not established.

Two carbogen-breathing animals with disseminated peritoneal disease arising from HCT-8 cancer cells were also studied. Results were generally similar to the HT29 tumors; featuring reduced ^{18}F -FDG uptake and pimonidazole binding coupled with unchanged GLUT-1 expression (compare supplementary figures 1 and 2).

For sub-millimeter-sized tumors, quantitative analysis showed that ^{18}F -FDG uptake was significantly lower for carbogen-breathing than for air-breathing for both tumor cell lines (Fig. 4D, Suppl. Fig. 3). The ratio of %ID/g ^{18}F -FDG uptakes between air and carbogen conditions was 2.5 ± 0.5 for HT29 (9 tumors from 2 air-breathing animals; 11 tumors from 2 carbogen-breathing animals) and 2.6 ± 0.2 for HCT-8 (3 tumors from 1 air-breathing animal; 6 tumors from 1 carbogen-breathing animal).

Discussion

We have previously reported the existence of severe hypoxia in microscopic tumors derived from HT29 and HCT-8 colorectal cancer cells grown intraperitoneally in nude mice (15,16). The current study confirms these findings and extends them to include the use of the PET tracer ^{18}F -FDG. In all cases there was a clear qualitative agreement between the level of ^{18}F -FDG uptake and the degree of binding of the hypoxia marker pimonidazole, suggesting a strong association between ^{18}F -FDG uptake and physiological hypoxia. In air-breathing animals, enhanced ^{18}F -FDG uptake was also associated with high expression of GLUT-1, but this was not maintained in the case of carbogen breathing. Relatively short-term carbogen breathing was effective in reducing physiological hypoxia in microscopic tumors, as evidenced by reduced pimonidazole binding, but had no obvious effect on the level of GLUT-1 expression. The observation that carbogen breathing also significantly reduced the uptake of ^{18}F -FDG is strong evidence that while high GLUT-1 expression may be necessary, it was not sufficient to ensure high ^{18}F -FDG uptake. In the tumor models used in this study, physiological hypoxia was also necessary for high ^{18}F -FDG uptake.

These results are consistent with previously published work on the relationship between hypoxia, glucose demand and FDG uptake *in-vitro* [reviewed in (2)]. Clavo et al (7) showed that ^3H -FDG uptake in HTB 63 melanoma and HTB 77 IP3 ovarian carcinoma cell lines was increased in hypoxic conditions in a time- and O_2 concentration-dependent manner. This appeared to be partly due to increased membrane expression of GLUT-1. In contrast, Burgman et al (5) found that hypoxia increased ^3H -FDG uptake in MCF7 breast carcinoma cells without any increase in either glucose transporter protein or hexokinase. In this case, the increase in ^3H -FDG uptake was attributed to an increase in glucose transporter activity due to hypoxia-induced alterations in cellular redox state. Our observation of significant changes in ^{18}F -FDG uptake between air- and carbogen-breathing coupled with no apparent changes in GLUT-1 expression is more supportive of the mechanism proposed by Burgman et al. Although it is possible that changes in hexokinase activity may also be involved, Waki et al found there was no correlation between hexokinase activity and ^3H -2-deoxyglucose uptake for 16 tumor cell lines (19).

Our results also agree with some *in-vivo* studies using macroscopic tumors, that showed a spatial correlation between the intratumoral distribution of ^{18}F -FDG and those of the hypoxic marker pimonidazole (9,13) and the expression of GLUT-1 (also GLUT-3 and hexokinase-II) (4). It has been noted (13) that differences between ^{18}F -FDG uptake in oxic and hypoxic regions would be reduced for tumors with high levels of aerobic glycolysis; a characteristic feature of cancer (20). This is because both anaerobic and aerobic glycolysis are inefficient sources of cellular energy (in comparison to oxidative phosphorylation) and both have a high demand for glucose. In the current study, using the human colorectal cancer cell lines HT29 and HCT-8, a carbogen-induced decrease in tumor hypoxia led to a significant reduction in ^{18}F -FDG accumulation. This suggests that these cells were able to down-regulate glycolysis in the newly oxygenated environment and that this change occurred rapidly, before noticeable alteration of GLUT-1 expression.

The finding that carbogen breathing-mediated reoxygenation produced a rapid decrease in tumor ^{18}F -FDG uptake raises some issues of potential clinical significance. In particular, the use of changes in ^{18}F -FDG tumor uptake to monitor response to cancer therapy may be subject to complications of interpretation due to treatment-induced changes in tumor hypoxic status. Additionally, oxygen breathing at the time of ^{18}F -FDG administration may decrease uptake in patient tumors and should probably be avoided if possible. Finally, although we found that microscopic peritoneal and ascites tumors were hypoxic with high ^{18}F -FDG uptake, it is unlikely that these could be visualized individually due to their small size. However it is possible that ensembles of microscopic tumors could be visualized. This may partly explain why malignant ascites may be evaluated by ^{18}F -FDG PET/CT as has recently been reported (21).

At a practical level, the disseminated peritoneal disease model used in this study has advantages over macroscopic subcutaneous xenografts as a system for examining mechanisms of radiotracer uptake. Macroscopic xenografts have a complex internal structure, with microscopic regions of aerobic, hypoxic and necrotic tumor together with normal stroma; all in close proximity. Consequently, when comparing digital autoradiograms with immunohistochemical images, problems may arise due to image mismatch. In contrast, individual microscopic tumors have a close to homogenous internal structure, e.g. either uniformly hypoxic and unperfused or oxygenated and well perfused. It is thus much easier to demonstrate that radiotracer autoradiograms match images of pimonidazole binding or hypoxia-regulated protein expression. A second advantage is that since a large number of peritoneal tumors (of differing size, hypoxic status, protein expression, etc.) can grow in an individual animal; it is possible to administer a radiotracer without confounding variations due to injected dose or inter-animal pharmacokinetics. Therefore, the disseminated peritoneal disease model is, at least, a valuable supplement to macroscopic xenograft models as a test system for radiotracer development.

We would also contend that the microscopic tumor model is of potential use for studying metastatic cancer, since microscopic tumors growing in animals may mimic some aspects of microscopic disease in patients. As most cancer-related deaths are due to the development of metastatic disease rather than the growth of primary tumors, the prevention or elimination of metastases before they become clinically detectable would be expected to reduce cancer mortality rates. However, if the pre-angiogenic phase of micrometastatic development involves an episode of severe hypoxia, the efficacy of adjuvant/neoadjuvant treatments in the form of chemotherapy and/or radiotherapy may be compromised by hypoxic resistance (15,16). If this is true, then new strategies will be required to meet the challenge, possibly with the aim of converting hypoxia into a target for systemic therapies. The high demand for glucose displayed by hypoxic micro-tumors suggests that glucose metabolism may be a suitable target for developing novel therapies for micrometastatic disease. Several

therapeutic strategies are under investigation to exploit or interrupt tumor glycolytic metabolism (22,23). Future studies to test the therapeutic efficacy of targeting glucose metabolism in micrometastatic model systems are warranted.

Conclusion

In a peritoneal model of disseminated microscopic disease, ^{18}F -FDG uptake was significantly increased in hypoxic microscopic tumors. This enhanced uptake could be abrogated by carbogen breathing. Physiological hypoxia was a necessary condition for increased ^{18}F -FDG uptake in microscopic tumors.

Supplementary Material

Refer to Web version on PubMed Central for supplementary material.

Acknowledgments

NIH grants R01 CA84596 and P01 CA115675, NCI grant P30-CA 08748.

Funding: This work was supported in part by NIH grants R01 CA84596 and P01 CA115675, and NCI grant P30-CA 08748

References

1. Ben-Haim S, Ell P. F-18-FDG PET and PET/CT in the Evaluation of Cancer Treatment Response. *J Nucl Med* 2009;50:88–99. [PubMed: 19139187]
2. Dierckx RA, Van de Wiele C. FDG uptake, a surrogate of tumour hypoxia? *Eur J Nucl Med Mol Imaging* 2008;35:1544–1549. [PubMed: 18509637]
3. Semenza GL. Targeting HIF-1 for cancer therapy. *Nat Rev Cancer* 2003;3:721–732. [PubMed: 13130303]
4. Zhao S, Kuge Y, Mochizuki T, et al. Biologic correlates of intratumoral heterogeneity in ^{18}F -FDG distribution with regional expression of glucose transporters and hexokinase-II in experimental tumor. *J Nucl Med* 2005;46:675–682. [PubMed: 15809491]
5. Burgman P, O'Donoghue JA, Humm JL, Ling CC. Hypoxia-Induced increase in FDG uptake in MCF7 cells. *J Nucl Med* 2001;42:170–175. [PubMed: 11197971]
6. Busk M, Horsman MR, Kristjansen PE, van der Kogel AJ, Bussink J, Overgaard J. Aerobic glycolysis in cancers: implications for the usability of oxygen-responsive genes and fluorodeoxyglucose-PET as markers of tissue hypoxia. *Int J Cancer* 2008;122:2726–2734. [PubMed: 18351643]
7. Clavo AC, Brown RS, Wahl RL. Fluorodeoxyglucose uptake in human cancer cell lines is increased by hypoxia. *J Nucl Med* 1995;36:1625–1632. [PubMed: 7658223]
8. Hara T, Bansal A, DeGrado TR. Effect of hypoxia on the uptake of [methyl- ^3H]choline, [1- ^{14}C]acetate and [^{18}F]FDG in cultured prostate cancer cells. *Nucl Med Biol* 2006;33:977–984. [PubMed: 17127170]
9. Pugachev A, Ruan S, Carlin S, et al. Dependence of FDG uptake on tumor microenvironment. *Int J Radiat Oncol Biol Phys* 2005;62:545–553. [PubMed: 15890599]
10. Tanaka T, Furukawa T, Fujieda S, Kasamatsu S, Yonekura Y, Fujibayashi Y. Double-tracer autoradiography with Cu-ATSM/FDG and immunohistochemical interpretation in four different mouse implanted tumor models. *Nucl Med Biol* 2006;33:743–750. [PubMed: 16934693]
11. Zanzonico P, Campa J, Polycarpe-Holman D, et al. Animal-specific positioning molds for registration of repeat imaging studies: comparative microPET imaging of F18-labeled fluorodeoxyglucose and fluoro-misonidazole in rodent tumors. *Nucl Med Biol* 2006;33:65–70. [PubMed: 16459260]
12. Bentzen L, Keiding S, Horsman MR, Falborg L, Hansen SB, Overgaard J. Feasibility of detecting hypoxia in experimental mouse tumours with ^{18}F -fluorinated tracers and positron emission

- tomography--a study evaluating [18F]Fluoro-2-deoxy-D-glucose. *Acta Oncol* 2000;39:629–637. [PubMed: 11093372]
13. Busk M, Horsman MR, Jakobsen S, Bussink J, van der Kogel A, Overgaard J. Cellular uptake of PET tracers of glucose metabolism and hypoxia and their linkage. *Eur J Nucl Med Mol Imaging* 2008;35:2294–2303. [PubMed: 18682937]
 14. Scigliano S, Pinel S, Poussier S, et al. Measurement of hypoxia using invasive oxygen-sensitive electrode, pimonidazole binding and 18F-FDG uptake in anaemic or erythropoietin-treated mice bearing human glioma xenografts. *Int J Oncol* 2008;32:69–77. [PubMed: 18097544]
 15. Li XF, Carlin S, Urano M, Russell J, Ling CC, O'Donoghue JA. Visualization of hypoxia in microscopic tumors by immunofluorescent microscopy. *Cancer Res* 2007;67:7646–7653. [PubMed: 17699769]
 16. Li XF, O'Donoghue JA. Hypoxia in microscopic tumors. *Cancer Lett* 2008;264:172–180. [PubMed: 18384940]
 17. Sobhanifar S, Aquino-Parsons C, Stanbridge EJ, Olive P. Reduced expression of hypoxia-inducible factor-1alpha in perinecrotic regions of solid tumors. *Cancer Res* 2005;65:7259–7266. [PubMed: 16103077]
 18. Li XF, Sun X, Ma Y, et al. Detection of hypoxia in microscopic tumors using ¹³¹I-labeled iodoazomycin galactopyranoside (¹³¹I-IAZGP) digital autoradiography. *Eur J Nucl Med Mol Imaging*. In press.
 19. Waki A, Kato H, Yano R, et al. The importance of glucose transport activity as the rate-limiting step of 2-deoxyglucose uptake in tumor cells in vitro. *Nucl Med Biol* 1998;25:593–597. [PubMed: 9804039]
 20. Heiden MG, Cantley LC, Thompson CB. Understanding the Warburg Effect: The Metabolic Requirements of Cell Proliferation. *Science* 2009;324:1029–1033. [PubMed: 19460998]
 21. Zhang M, Jiang X, Zhang M, Xu H, Zhai G, Li B. The Role of 18F-FDG PET/CT in the evaluation of Ascites of Undetermined Origin. *J Nucl Med* 2009;50:506–512. [PubMed: 19289438]
 22. Gatenby RA, Gillies RJ. Glycolysis in cancer: A potential target for therapy. *Int J Biochem Cell Biol* 2007;39:1358–1366. [PubMed: 17499003]
 23. Sheng HM, Niu B, Sun HB. Metabolic Targeting of Cancers: From Molecular Mechanisms to Therapeutic Strategies. *Curr Med Chem* 2009;16:1561–1587. [PubMed: 19442134]

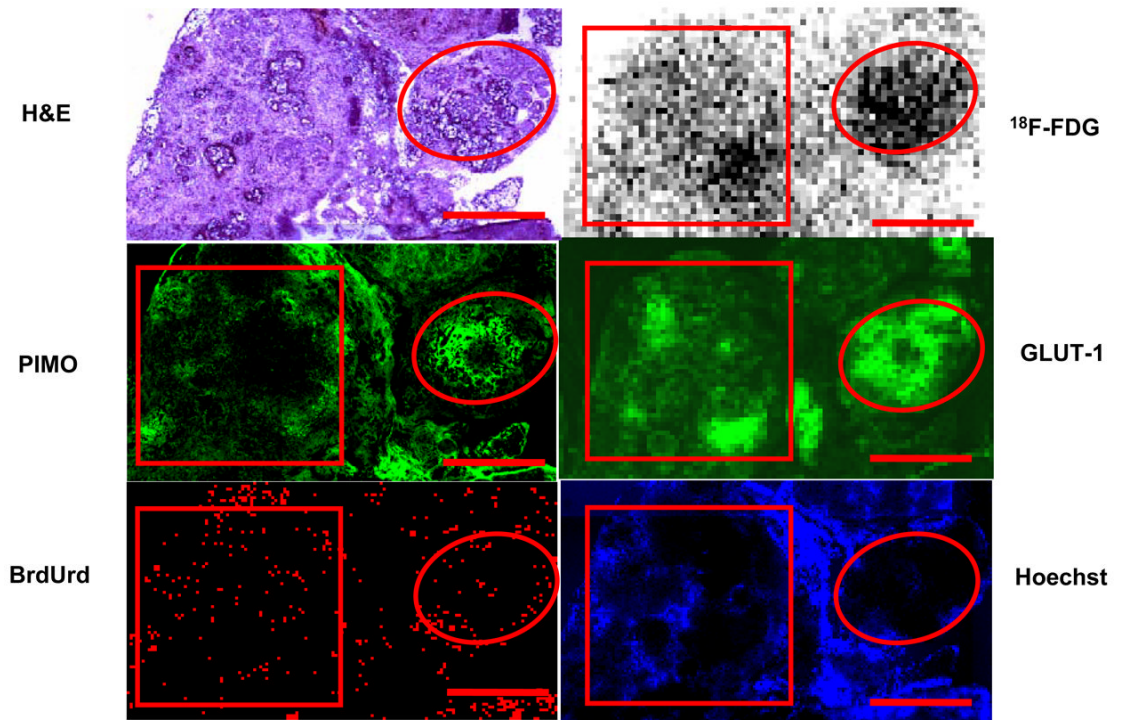


Figure 1. ^{18}F -FDG uptake in HT29 peritoneal tumors in air breathing condition. Part of a larger tumor (square) has relatively low levels of ^{18}F -FDG uptake, PIMO binding, and GLUT-1 expression, with relatively high levels of cell proliferation and blood perfusion. A microscopic tumor (circle) has relatively high FDG uptake, PIMO binding and GLUT-1 with lower cell proliferation and little perfusion. Similar results were seen in 7 animals. Scale bar 1 mm.

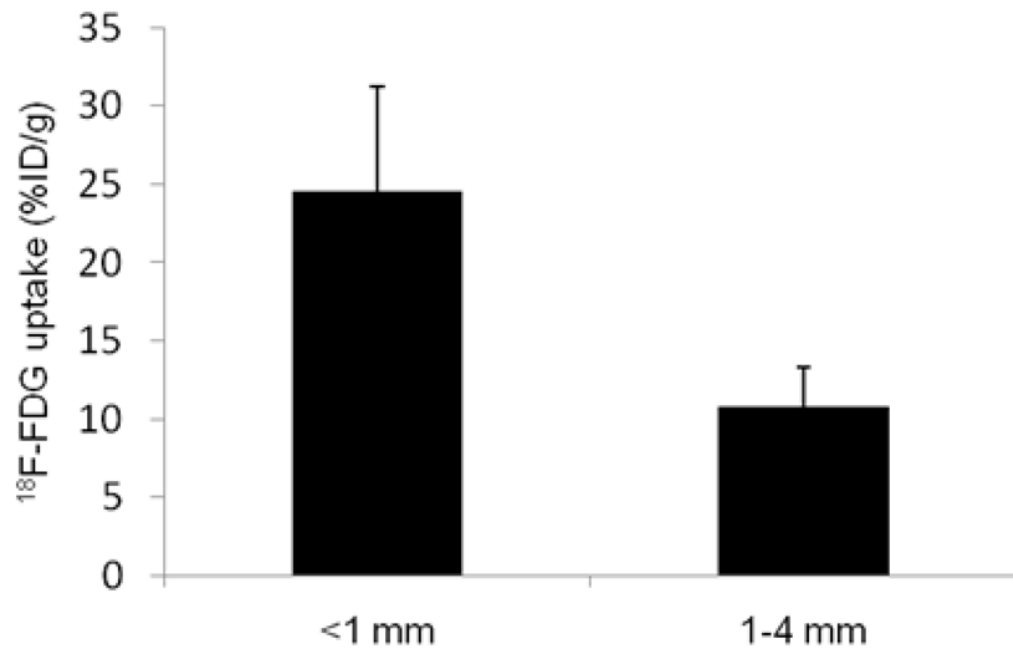


Figure 2. Quantitative ^{18}F -FDG uptake based on a collection of intraperitoneal HT29 tumors derived from 5 tumors (<1mm diameter) and 4 tumors (1–4mm diameter), all from a single air-breathing. ^{18}F -FDG uptake was significantly higher in smaller tumors than larger ones, $P < 0.001$.

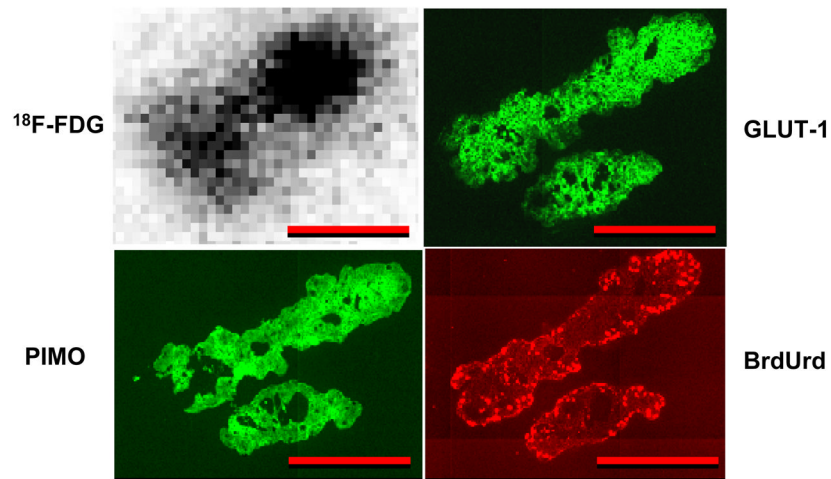


Figure 3. Comparison of ^{18}F -FDG uptake with tumor hypoxia, GLUT-1 expression and cellular proliferation in 2 HT29 ascites tumors from an air-breathing animal. Ascites tumors had high ^{18}F -FDG uptake, pimonidazole binding and GLUT-1 expression with proliferation (BrdUrd) confined to the rim. Scale bar 500 μm .

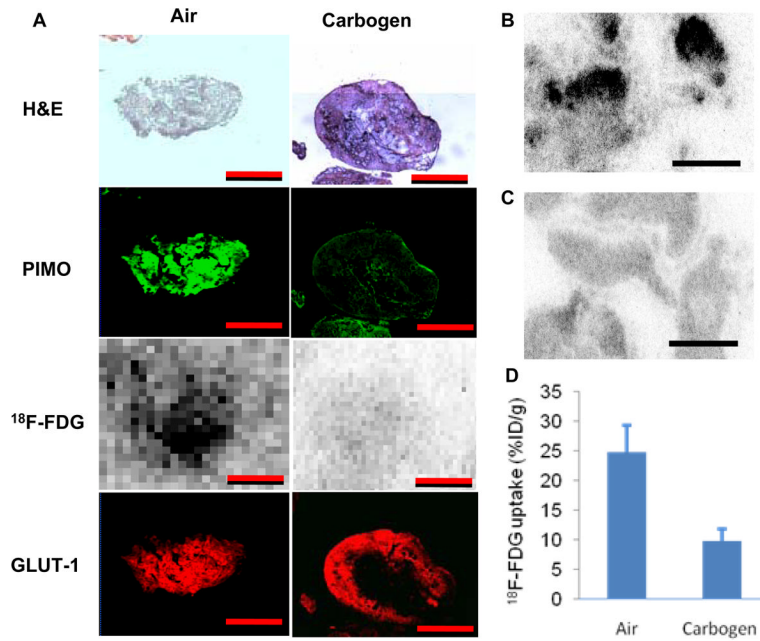


Figure 4.

(A) Comparison of HT29 peritoneal tumors from animals breathing air or carbogen (95% O₂, 5% CO₂). ¹⁸F-FDG uptake and pimonidazole binding were markedly reduced for carbogen breathing whereas GLUT-1 expression was unaffected (see text for details). Scale bar 500 μm. (B) For air breathing conditions, overall ¹⁸F-FDG uptake was higher and a number of “hot spots” were observed. In contrast, carbogen breathing (C) resulted in significantly less ¹⁸F-FDG uptake in microscopic tumors. Similar results were seen in 4 carbogen-breathing animals. Scale bars 4 mm. (D) The difference in ¹⁸F-FDG uptake between sub-millimeter HT29 tumors in air-breathing (9 tumors from 2 animals) and carbogen-breathing (11 tumors from 2 animals) animals was significant p<0.001.